Characterization of the Content and Distribution of Collagen and Proteoglycan in the Decellularized Book-Shaped Enthesis Scaffolds by SR-FTIR

Hongbin Lu
Xiangya Hospital Central South University
qiang shi
Xiangya Hospital Central South University
Can Chen
Xiangya Hospital Central South University
Muzhi Li
Xiangya Hospital Central South University
Yang Chen
Xiangya Hospital Central South University
Yan Xu
Xiangya Hospital Central South University
Jianzhong Hu (jianzhonghu@hotmail.com)
https://orcid.org/0000-0001-5903-7172

Research article

Keywords: SR-FTIR, Decellularized book-shaped enthesis scaffolds, Bone-tendon interface, Rabbit rotator cuff

Posted Date: June 16th, 2020

DOI: https://doi.org/10.21203/rs.3.rs-32047/v1

Version of Record: A version of this preprint was published on March 1st, 2021. See the published version at https://doi.org/10.1186/s12891-021-04106-x.

Abstract

Background: Bone-tendon interface (enthesis) plays a pivotal role in relaxing load transfer between otherwise structurally and functionally distinct tissue types. Currently, decellularized extracellular matrix (DEM) from enthesis provide a natural three-dimensional scaffold with tissue-specific orientations of extracellular matrix molecules for enthesis regeneration, however, the content and distribution of collagen and proteoglycan in the decellularized book-shaped enthesis scaffolds from rabbit rotator cuff by SR-FTIR have not been reported.

Methods: Native enthesis tissues (NET) harvested from rabbit rotator cuff were sectioned into cuboid (about 30 mm × 1.2 mm × 10 mm) for decalcified. The decellularized book-shaped enthesis scaffolds were conducted and intrinsic ultrastructure was evaluated by histological staining and scanning electron microscopy (SEM), respectively. The content and distribution of collagen and proteoglycan in the decellularized book-shaped enthesis scaffolds from rabbit rotator cuff were also measured innovatively by SR-FTIR.

Results: The decellularized book-shaped enthesis scaffolds from rabbit rotator cuff were successfully obtained. Histomorphology and SEM evaluated the decellularized effect and the structure of extracellular matrix during decellularization. After mechanical test, we found the failure load in the NET group was higher than that in the DEM group ($P < 0.05$), reached 1.32 times as much as that in the DEM group. Meanwhile, the stiffness of the DEM group was significantly lower than the NET group. Furthermore, the distributions of collagen and PGs content in the decellularized book-shaped enthesis scaffolds were decreased obviously after decellularization by SR-FTIR quantitative analysis.

Conclusion: SR-FTIR was applied innovatively to characterize the histological morphology of native enthesis tissues from rabbit rotator cuff. Moreover, it can be used for quantitative mapping of the content and distribution of collagen and PGs content in the decellularized book-shaped enthesis scaffolds.

Background

Bone-tendon interface (BTI), which is also named as enthesis, serves as an interface for force transmission from bone to tendon that consists of four transitional tissues: tendon, uncalcified fibrocartilage, calcified fibrocartilage, and bone [1, 2]. This transitional enthesis allows smooth transmission of forces derived from muscle contraction and minimize formation of stress peaks [3, 4]. Enthesis injury, particularly those in the rotator cuff, are prevalent conditions which often lead to disability and persistent pain [5]. Regrettably, rapid and functional enthesis regeneration remains difficult because of its poor capacity of self-repair during healing [6-8]. Thus, conventional surgical treatment, only attaching the ruptured tendon and bony footprint together, cannot recapitulate the enthesis with graded and transitional structure, thus resulting in a high rate of re-rupture (20-94%) [1, 9].

With the development of tissue engineering technology, decellularized bioscaffolds have received great attention due to their ability to enhance tissue regeneration and repair damaged tissues [10-12]. Previous

studies indicated that organ-specific extracellular matrix scaffolds derived from site-specific homologous tissues may be better suited for constructive tissue remodeling than no site-specific tissue sources. As a result, decellularized extracellular matrix from enthesis may provide a natural three-dimensional scaffold with tissue-specific orientations of extracellular matrix molecules for enthesis regeneration. Recently, synchrotron radiation-based fourier transform infrared microspectroscopy (SR-FTIR) has been proved to be a useful tool for the analysis of complex components in biological samples [13]. In our previous studies, the application of SR-FTIR for quantitative evaluation of GAG and collagen in book-shaped decellularized fibrocartilage scaffold has been reported [14]. Zhou et al. found that SR-FTIR could be used as a tool for quantitative mapping of the content and distribution of extracellular matrix in the cellularized or decellularized bioscaffolds and it could provide a new platform for quantitative evaluation of extracellular matrix in decellularized bioscaffolds [15].

The surgical outcome in small-animal experiments, such as mice, may not be replicable in large animals owing to differences in joint anatomy (structure) and function (mechanics) [3]. Furthermore, the healing ability of small animals is often faster than that of large animals or humans. Hence, the rabbit models of BTI healing that mimics the mechanical loading and healing ability of humans to evaluate a variety of new strategies for the treatment of rotator cuff tears is desirable [16]. Additionally, Mathewson et al. [17] compared rotator cuff muscle architecture of several animal models with that of humans and demonstrated that rabbit muscular parameters were more similar to humans than that in other large animals. However, to date, the application of SR-FTIR for quantitative evaluation of extracellular matrix components in decellularized book-shaped enthesis scaffolds from rabbit rotator cuff has not been reported.

In this study, we aimed to apply SR-FTIR as a tool for quantitative mapping of the content and distribution of extracellular matrix in the decellularized book-shaped enthesis scaffolds from rabbit rotator cuff, so as to verify the decellularized method conducted by Su M et al' protocol which could shorten decellularized time, well preserve the native structure, extracellular matrix components and mechanical properties of enthesis tissue [18].

Methods

Preparation of NET samples and decellularized book-shaped enthesis scaffolds

The experiment design is illustrated as in **Fig. 1**. In total, 32 female New Zealand rabbits weighing 3.1 ± 0.3 kg (supplied by the Experimental Animal Center of Central South University, Changsha, China) were euthanized (intraperitoneal injection of sodium pentobarbital, 100 mg/kg) in this study and NET harvested from the supraspinatus were sectioned into cuboid (about 30 mm × 1.2 mm × 10 mm) for decalcified and then vertically sliced at the boundary between fibrocartilage and tendon. The specimens were sectioned into book shape from the tendinous end to bony end along myotility direction with layer thicknesses of 250 μm. Layers 250 μm in thickness were selected for preparing book-shaped scaffold and the DEM was conducted by Su M et al' protocol.

Histology and scanning electron microscopy (SEM) analysis

Hematoxylin and eosin (H&E), toluidine blue fast green and 4',6-diamidino-2-Phenyl

indole (DAPI) for histological observation was used to evaluate decellularized efficacy (N=3). The decellularized book-shaped enthesis scaffolds from rabbit rotator cuff were embedded in paraffin and sectioned into 7 μm slices, then staining with HE, toluidine blue fast green and DAPI for observing the retention of nuclear materials. The samples (N=3) used for SEM scanning were fixed with 2.5% glutaraldehyde for 24 h and then washed with PBS, dehydrated by gradient ethanol, and soaked with isoamyl acetate. The microstructure of the decellularized book-shaped enthesis scaffolds surface was observed and the decellularized components was detected.

SR-FTIR analysis

In this study, we innovatively applied the synchrotron radiation-Fourier transform infrared spectroscopy (SR-FTIR) to comparatively evaluate the preservation of collagen and PGs in the NET and DEM (N=3). The result of decellularization on the extracellular matrix components were evaluated using synchrotron radiation-Fourier transform infrared spectroscopy (SR-FTIR) at the BL01B beamline of National Facility for Protein Science Shanghai and Shanghai Synchrotron Radiation Facility, where synchrotron radiation from a bending magnet was collected, collimated and transported to a commercial FTIR interferometer bench. The peak area of amide I (1720-1590 cm-1) and carbohydrate (1140-985 cm-1) in the infrared spectrum were respectively calculated to characterize the distribution and content of collagen and PGs of the NET or DEM. The specifical procedures are as previously described according to the published literature [19].

DNA content analysis and mechanical tests

The quantifications of DNA in the decellularized book-shaped enthesis scaffolds were performed using DNeasy Blood & Tissue protocol according to the manufacturer's instructions [12]. Specifically, the decellularized book-shaped enthesis scaffolds (N=3) were weighed and minced after freeze-dried for 24 h using a lyophilizer (SIM International Group, USA). Then the decellularized bone-tendon scaffold (10 mg) was digested with proteinase K at 56℃ for 3 h. Finally, the DNA content in the decellularized book-shaped enthesis scaffolds was quantified by DNeasy Blood&Tissue Kit (Qiagen, USA) together with PicoGreen DNA assay kit (Invitrogen, USA).

The mechanical properties of the NET and DEM were comparatively evaluated with mechanical testing system (preloaded: 1 N, tension rate: 20 mm min^{-1}, 23 MTS Insight, MTS, USA) (N=3). The mechanical index should be included as follows: failure load and stiffness.

Attachment and Viability Assay

After washing for three times with PBS (3 × 30 min), the decellularized book-shaped enthesis scaffolds were sterilized and immersed in complete medium overnight, then 10^4 BMSCs were respectively seeded

onto the decellularized book-shaped enthesis scaffolds. To evaluate the cytotoxicity of the decellularized book-shaped enthesis scaffolds on BMSCs, cell viability was evaluated with a Live/Dead Assay kit (Invitrogen) at day 3 after seeding, Live/Dead assay showed that the green- and red-stained cells were captured by fluorescence with excitation wavelength of 488/594 nm to quantify cell viability (N=3).

Statistical analysis

All statistical analyses were performed using SPSS software (Version 23.0, Chicago, USA). Data was expressed as mean ± standard deviation. Statistical significance of the experimental variables was then evaluated using Student's t-test ($P < 0.05$ was considered statistically significant).

Results

Characterization of thedecellularized book-shaped enthesis scaffolds by macroscopic observation and histomorphology

In this study, enthesis tissue was sectioned into "book" shape along myotility direction with thickness of 250 um (**Fig. 2A)**. H&E, Toluidine blue fast green, Dapi staining were used together to evaluate the decellularized effect. H&E and Toluidine blue fast green staining showed that the cellular components of the decellularized book-shaped enthesis scaffolds were absolutely removed, while the structure and morphology of the native enthesis extracellular matrix were well preserved (**Fig. 2B, C**). In addition, Dapi-positive cell nuclei were rarely showed in the decellularized book-shaped enthesis scaffolds (**Fig. 2D**).

SEM analysis

SEM was used to detect the surface topology of book-shaped enthesis scaffolds before or after decellularization (**Fig. 3**). In the native book-shaped enthesis scaffolds, cells were adhered to various native tissues. After decellularization, no cellular components were observed on the surface of the scaffold while the native the collagen fibers were well preserved.

Distribution and content of collagen and proteoglycan by SR-FTIR

Collagen and proteoglycan contents were estimated by integrating the peak area under the Amide I band (1720-1590 cm-1) and C-O-C and C-OH vibrations (1140-985 cm-1), respectively. The mappings were collected by OMNIC 9 software (Thermo Fisher Scientific) and five points of each sample were selected randomly for semi-quantitative analysis. In this study, we innovatively applied SR-FTIR to comparatively characterize the distribution and content of collagen and proteoglycan among NET and DEM. As presented in Fig. 4 (N=3), the collagen content in the DEM lost about 40.85% (Fig. 4D). Meanwhile, SR-FTIR analysis indicated that the PGs distribution at DEM were partly reserved after decellularization, its content decreased about 44.55% in the DEM (Fig. 4E).

DNA residence and mechanical test

After decellularization, the content of DNA was greatly reduced (0.976 ± 0.018 μg/mg) in the DEM, which was significantly lower than that in the NET (0.089 ± 0.026 μg/mg) ($P < 0.05$) (**Fig. 5A**). The failure load and stiffness of two groups were obtained by biomechanical examination. After mechanical test, we found the failure load in the DET group was higher than that in the DEM group ($P < 0.05$), reached 1.32 times as much as that in the DEM group (**Fig. 5B**). Meanwhile, the stiffness of the DEM group was significantly lower than the DET group (**Fig. 5C**).

Biological characteristics of DEMon BMSCs viability

To evaluate the effects of DEM on BMSCs viability, Live/Dead assay were used to examine cell proliferation and viability of BMSCs cultured on the DEM. At day 3 after seeding, Live/Dead assay showed that most BMSCs were stained fluorescent green (living cells), with very few red (dead cells) (**Fig. 6**).

Discussion

The rotator cuff repair, which often leads to disability and persistent pain, is very common in the shoulder and the bone-tendon interface healing is crucial to regenerate native fibrocartilaginous structure. Howover, this unique tissue structure healing remains difficult because of the limited ability of tendons to self-repair [6]. To improve the healing of bone-tendon interface, tissue engineering has been widely examined in this field, utilizing a combination of scaffolds, bioactive molecules and seed cells to repair damaged tissues.

Decellularization technology has been widely used to obtain decellularized scaffolds, such as decellularized bone, fibrocartilage, or tendon tissue. There are two crucial steps during decellularization: removing cell component and preserving the extracellular matrix components. Collagen and proteoglycan are two important biocomponents in the extracellular matrix and the main structures of bone, fibrocartilage, and tendon extracellular matrix are composed of different types of collagen [20]. In our previous study, Chen et al. applied book-shaped decellularized fibrocartilage scaffold for bone-tendon healing in patella patellar-tendon complexes and achieved better results [14]. Nevertheless, few decellularization methods, which not only well removed cell component and preserved the whole natural structure and mechanical properties, is available for the large-size enthesis scaffold. Recently, Su M et al developed an decellularized protocol for porcine enthesis decellularization, which includes the processes of tissue-trimming, freeze-thaw cycles, 3%SDS, and nuclease digestion. However, whether the contents and distribution of collagen fiber and proteoglycan could be reserved still needs to be explored.

With the development of the third generation synchrotron light source Shanghai Synchrotron Radiation Facility (SSRF), the SR-FTIR (higher spatial resolution of 5 μm) has been applied to analysis at the diffraction limit while preserving a high spectral quality [13]. The flux at the entrance of the SR-FTIR spectrometer has been achieved to be about 1.5×10^{13} (photons/sec/0.1% b.w.) at 1 μm wavelength for a 230 mA current. These performances allow the SR-FTIR to analysis large samples with heterogeneous

regions in a small area with a diffraction limited spatial resolution [21]. This study utilizes SR-FTIR as it is a high-throughput and sensitive imaging modality which is capable of quantitative mapping of the content and distribution of extracellular matrix, thereby making it well suited for examining multi-tissue regions. Compared with the conventional FTIR, the SR-FTIR can detect the changes in microstructure in high resolution, and determine the various components of the decellularized book-shaped enthesis scaffolds.

Meanwhile, utilizing SR-FTIR technique, both collagen, proteoglycan, as well as collagen orientation, were detected and quantified across the different regions of the decellularized book-shaped enthesis scaffolds. The extent of decellularization on extracellular matrix of the bone-tendon scaffolds can be assessed by such structural chemical information. Evaluating these compositional changes is crucial to elucidating the role of the bioscaffolds in rabbit rotator cuff [22]. For the first time, SR-FTIR technology was used to reveal the microstructure of the extracellular matrix and the quality of decellularized book-shaped enthesis scaffolds in rabbit rotator cuff. In the present study, we analyzed the absorption intensity of collagen and proteoglycan, plotted the chemical maps of the samples, and quantitatively analyzed the content and distribution of extracellular matrix in the decellularized book-shaped enthesis scaffolds. As shown in our results, 40.85% collagen and 44.55% proteoglycan is lost after decellularization. Our findings provide critical information for the regeneration of bone-tendon interface and new insights into matrix composition and organization across the decellularized bone- tendon scaffold. To prove this interpretation, we should increase the number of samples and study other types of BTI in follow-up experiments.

This present study focused on quantitative mapping of changes in matrix components across the decellularized large-size enthesis tissue as scaffolds using the SR-FTIR technology and the results indicated a novel decellularized protocol for large-size enthesis, which obviously shortened decellularized time, well preserved the native structure, extracellular matrix components and mechanical properties of enthesis tissue should be developed in future.

Assessing the matrix components of decellularized meniscus and cartilage extracellular matrix by the SR-FTIR technology are the next steps in the following studies. The future application of SR-FTIR would be extended to observe mineral distributions and potentially facilitate the understanding the transition of complex loads from bone to ligament.

Conclusion

In summary, the goal of this study is to utilize SR-FTIR to analyze the content and distribution of collagen and proteoglycan in the decellularized book-shaped enthesis scaffolds from rabbit rotator cuff. After following Su M et al' decellularization protocol, cell components were effectively removed and the microstructure of the scaffold was well preserved, however, changes in extracellular matrix components, such as collagen and proteoglycan, were observed. Therefore, a novel decellularized protocol for large-size enthesis, which obviously shortened decellularized time, well preserved the native structure,

extracellular matrix components and mechanical properties of enthesis tissue should be developed in future.

Abbreviations

BMSC: Bone marrow stromal cell; OCT: Optimum cutting temperature; SEM: Scanning electron microscopy; SR-FTIR: Synchrotron radiation-based Fourier transform infrared microspectroscopy; SSRF: Shanghai Synchrotron Radiation Facility; NET: Native enthesis tissues; DEM: decellularized enthesis matrix; BTI: Bone-tendon interface

Declaration

Ethics approval and consent to participate

All experimental procedures conformed to the guidelines in the Guide for the Care and Use of Laboratory Animals published by the Chinese National Health and were approved by the Ethics Committee of the Center for Scientific Research with Animal Models of Central South University (2019030517).

Consent for publication

Not applicable.

Availability of data and materials

The datasets supporting the conclusions of this article are included within the article. The raw data can be requested from the corresponding author on reasonable request.

Competing interests

The authors declare that they have no competing interests.

Funding

This study was supported by the Fundamental Research Funds for the Central Universities of Central South University (Nos. 2019zzts900), and National Natural Science Foundation of China (NO. 81730068).

The Fundamental Research Funds for the Central Universities of Central South University and National Natural Science Foundation of China had no role in the study design, collection, analysis and interpretation of data nor in the writing of the manuscript and in the decision to submit the manuscript for publication.

Authors' contributions

CC conceived and designed the study. QS and YC completed the experiments. YX, and ML analyzed the data. HL and JH wrote the paper. All authors have read and approved the manuscript.

Acknowledgements

We thank the staffs from BL01B beamline of National Center for Protein Science Shanghai (NCPSS) for assistance during data collection.

References

1. Atesok K, Fu FH, Wolf MR, Ochi M, Jazrawi LM, Doral MN, Lubowitz JH, Rodeo SA: **Augmentation of tendon-to-bone healing**. *J Bone Joint Surg Am* 2014, **96**(6):513-521.
2. Derwin KA, Galatz LM, Ratcliffe A, Thomopoulos S: **Enthesis Repair: Challenges and Opportunities for Effective Tendon-to-Bone Healing**. *J Bone Joint Surg Am* 2018, **100**(16):e109.
3. Lu HH, Thomopoulos S: **Functional attachment of soft tissues to bone: development, healing, and tissue engineering**. *Annu Rev Biomed Eng* 2013, **15**:201-226.
4. Lu H, Chen C, Qu J, Chen H, Chen Y, Zheng C, Wang Z, Xu D, Zhou J, Zhang T *et al*: **Initiation Timing of Low-Intensity Pulsed Ultrasound Stimulation for Tendon-Bone Healing in a Rabbit Model**. *Am J Sports Med* 2016, **44**(10):2706-2715.
5. Zelzer E, Blitz E, Killian ML, Thomopoulos S: **Tendon-to-bone attachment: from development to maturity**. *Birth Defects Res C Embryo Today* 2014, **102**(1):101-112.
6. Benjamin M, Toumi H, Ralphs JR, Bydder G, Best TM, Milz S: **Where tendons and ligaments meet bone: attachment sites ('entheses') in relation to exercise and/or mechanical load**. *J Anat* 2006, **208**(4):471-490.
7. Hu J, Qu J, Xu D, Zhang T, Qin L, Lu H: **Combined application of low-intensity pulsed ultrasound and functional electrical stimulation accelerates bone-tendon junction healing in a rabbit model**. *J Orthop Res* 2014, **32**(2):204-209.
8. Xu D, Zhang T, Qu J, Hu J, Lu H: **Enhanced patella-patellar tendon healing using combined magnetic fields in a rabbit model**. *Am J Sports Med* 2014, **42**(10):2495-2501.
9. Galatz LM, Ball CM, Teefey SA, Middleton WD, Yamaguchi K: **The outcome and repair integrity of completely arthroscopically repaired large and massive rotator cuff tears**. *J Bone Joint Surg Am* 2004, **86**(2):219-224.
10. Wang L, Johnson JA, Zhang Q, Beahm EK: **Combining decellularized human adipose tissue extracellular matrix and adipose-derived stem cells for adipose tissue engineering**. *Acta Biomater* 2013, **9**(11):8921-8931.
11. Han TT, Toutounji S, Amsden BG, Flynn LE: **Adipose-derived stromal cells mediate in vivo adipogenesis, angiogenesis and inflammation in decellularized adipose tissue bioscaffolds**. *Biomaterials* 2015, **72**:125-137.

12. Guo L, Qu J, Zheng C, Cao Y, Zhang T, Lu H, Hu J: **Preparation and Characterization of a Novel Decellularized Fibrocartilage "Book" Scaffold for Use in Tissue Engineering**. *PLoS One* 2015, **10**(12):e0144240.
13. Kastyak-Ibrahim MZ, Nasse MJ, Rak M, Hirschmugl C, Del Bigio MR, Albensi BC, Gough KM: **Biochemical label-free tissue imaging with subcellular-resolution synchrotron FTIR with focal plane array detector**. *Neuroimage* 2012, **60**(1):376-383.
14. Chen C, Liu F, Tang Y, Qu J, Cao Y, Zheng C, Chen Y, Li M, Zhao C, Sun L *et al*: **Book-Shaped Acellular Fibrocartilage Scaffold with Cell-loading Capability and Chondrogenic Inducibility for Tissue-Engineered Fibrocartilage and Bone-Tendon Healing**. *ACS Appl Mater Interfaces* 2019, **11**(3):2891-2907.
15. Zhou Y, Chen C, Guo Z, Xie S, Hu J, Lu H: **SR-FTIR as a tool for quantitative mapping of the content and distribution of extracellular matrix in decellularized book-shape bioscaffolds**. *BMC Musculoskelet Disord* 2018, **19**(1):220.
16. Adams JE, Zobitz ME, Reach JS, Jr., An KN, Steinmann SP: **Rotator cuff repair using an acellular dermal matrix graft: an in vivo study in a canine model**. *Arthroscopy* 2006, **22**(7):700-709.
17. Mathewson MA, Kwan A, Eng CM, Lieber RL, Ward SR: **Comparison of rotator cuff muscle architecture between humans and other selected vertebrate species**. *J Exp Biol* 2014, **217**(Pt 2):261-273.
18. Su M, Zhang Q, Zhu Y, Wang S, Lv J, Sun J, Qiu P, Fan S, Jin K, Chen L *et al*: **Preparation of Decellularized Triphasic Hierarchical Bone-Fibrocartilage-Tendon Composite Extracellular Matrix for Enthesis Regeneration**. *Advanced Healthcare Materials* 2019, **8**(19).
19. Khanarian NT, Boushell MK, Spalazzi JP, Pleshko N, Boskey AL, Lu HH: **FTIR-I compositional mapping of the cartilage-to-bone interface as a function of tissue region and age**. *J Bone Miner Res* 2014, **29**(12):2643-2652.
20. Calejo I, Costa-Almeida R, Gomes ME: **Cellular Complexity at the Interface: Challenges in Enthesis Tissue Engineering**. *Adv Exp Med Biol* 2019, **1144**:71-90.
21. Zhang ZY, Chen M, Tong YJ, Ji T, Zhu HC, Peng WW, Zhang M, Li YJ, Xiao TQ: **Performance of the infrared microspectroscopy station at SSRF**. *Infrared Physics & Technology* 2014, **67**:521-525.
22. Spalazzi JP, Boskey AL, Pleshko N, Lu HH: **Quantitative mapping of matrix content and distribution across the ligament-to-bone insertion**. *PLoS One* 2013, **8**(9):e74349.

Figures

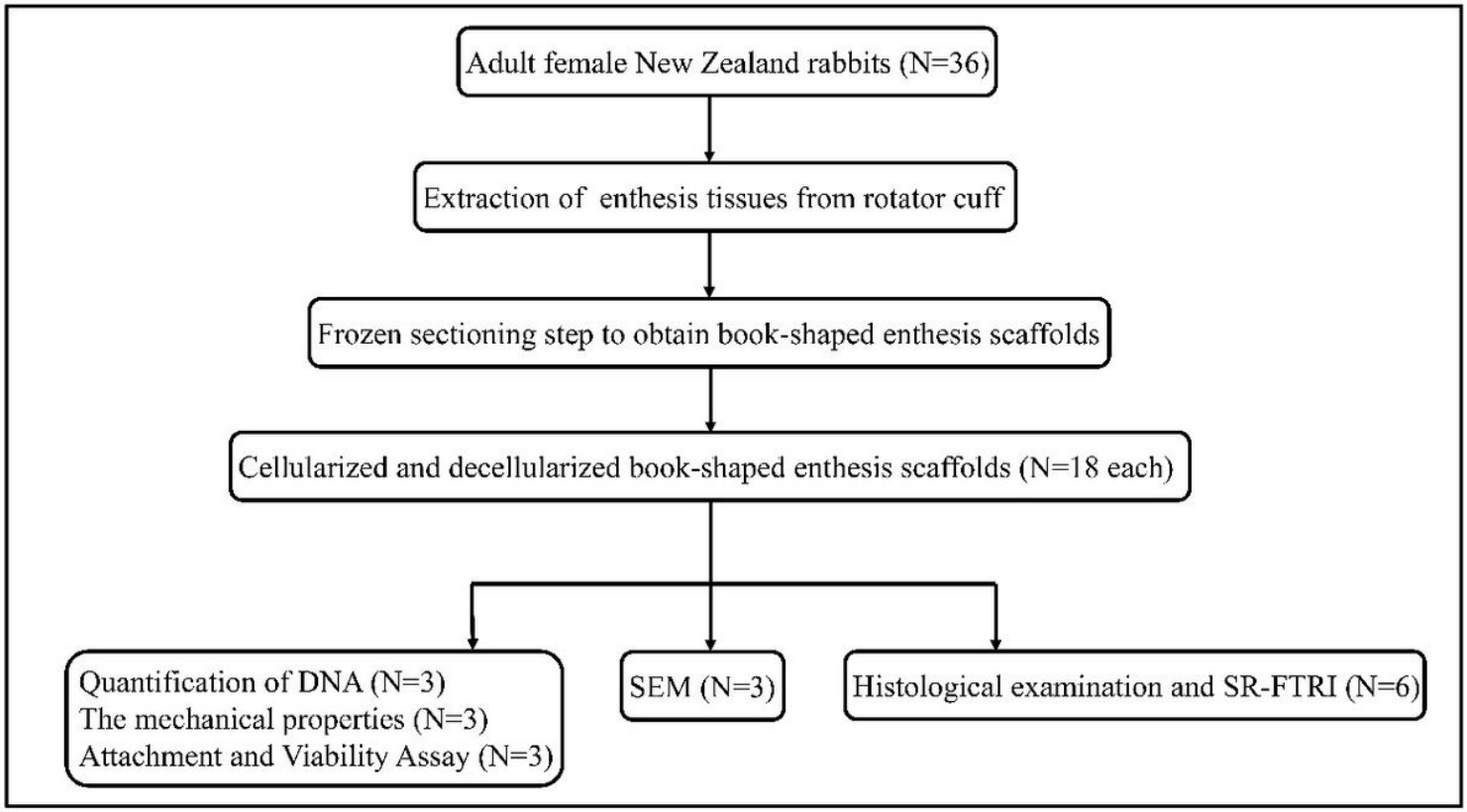

Figure 1

The technology roadmap of the experiment design

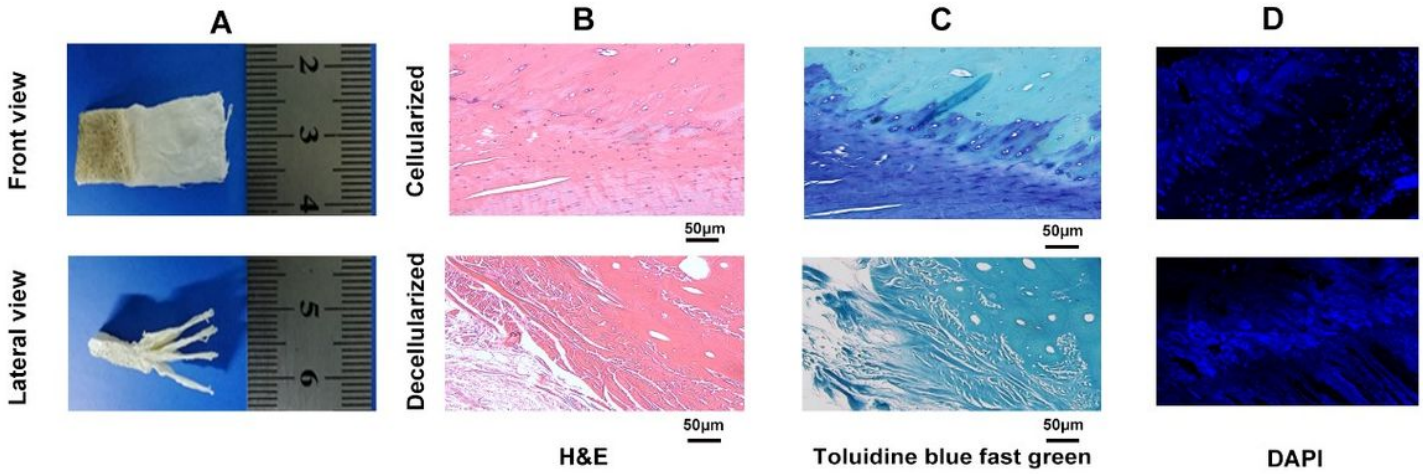

Figure 2

Characterization of the book-shaped enthesis scaffold. (A) The macroscopic observation of the decellularized book-shaped enthesis scaffold; (B) H&E staining, (C) Toluidine blue fast green staining, and (D) DAPI staining were used together to evaluate the decellularized effect in the decellularized book-shaped enthesis scaffold.

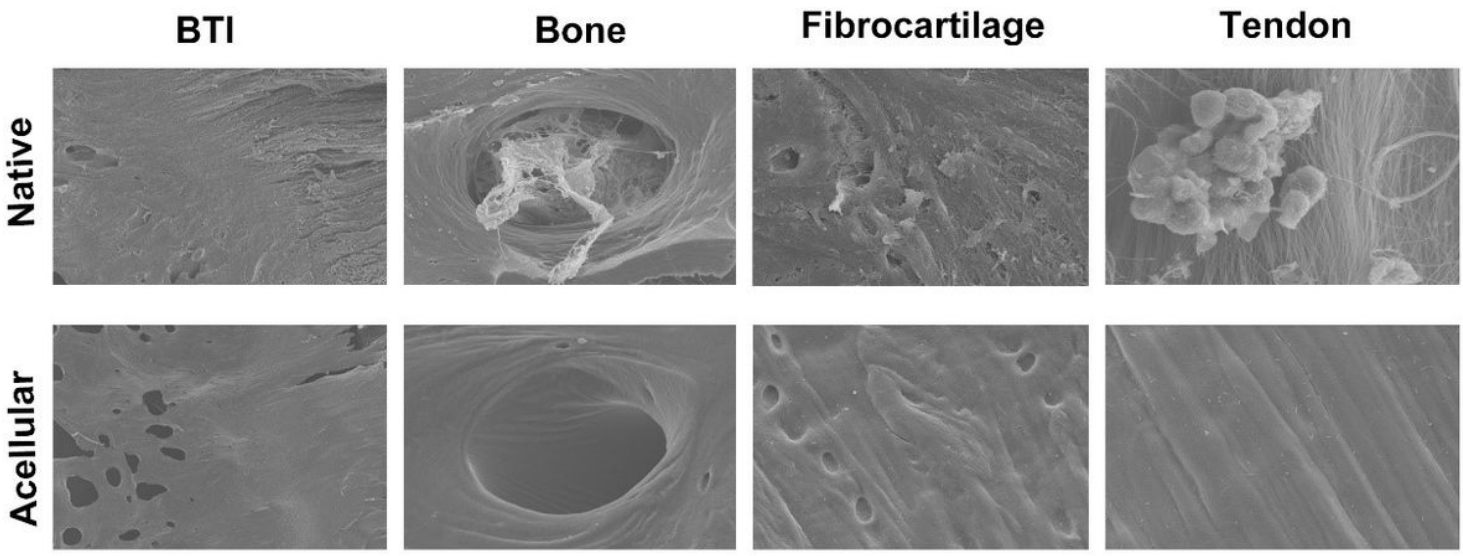

Figure 3

From the SEM image, the decellularized book-shaped enthesis scaffolds following Su M et al' protocol preserved native collagen structure well, and no cells debris were visualized.

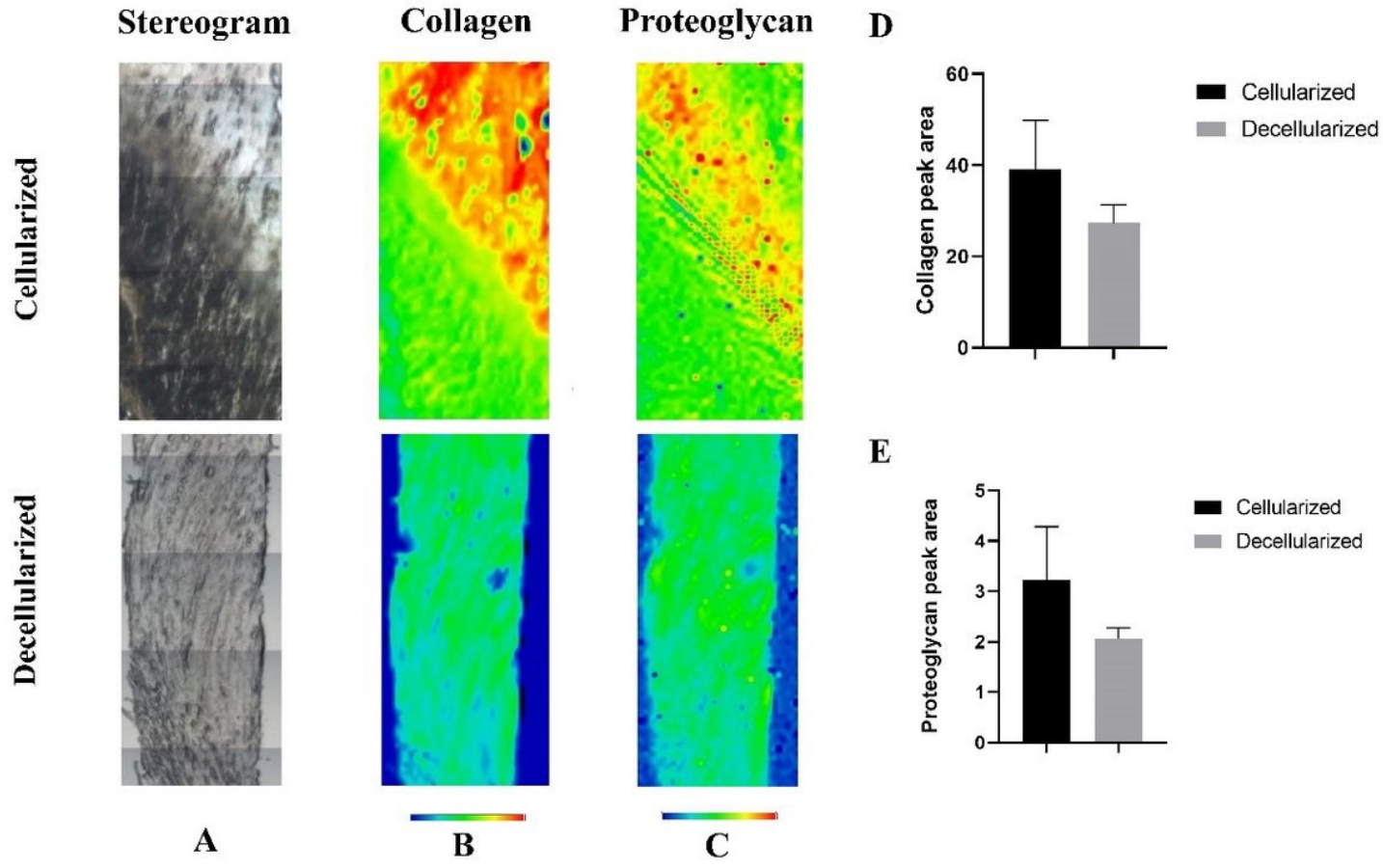

Figure 4

SR-FTIR mappings (Scale bar: 10 μm), including collagen and proteoglycan distribution, of the NET or DEM. A Light microscopy images. B Distribution of collagen. C Distribution of proteoglycan. D Content of collagen within the cellularized or decellularized book-shaped enthesis scaffolds. E Content of proteoglycan within the cellularized or decellularized book-shaped enthesis scaffolds. The results indicating a significant difference ($P < 0.05$)

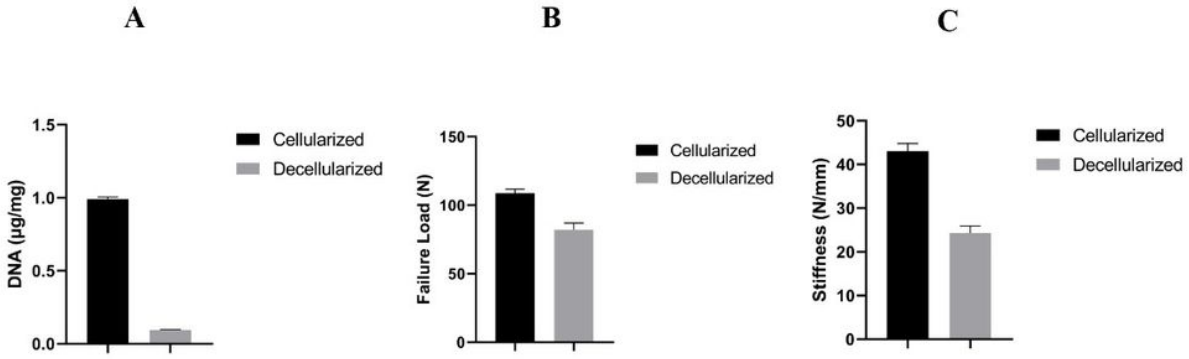

Figure 5

Quantification of DNA, failure load, and stiffness in the decellularized book-shaped enthesis scaffolds. A Content of DNA within the NET or DEM. B The mechanical properties (failure load). C The mechanical properties (stiffness). Dissimilar letters indicating a significant difference ($P < 0.05$)

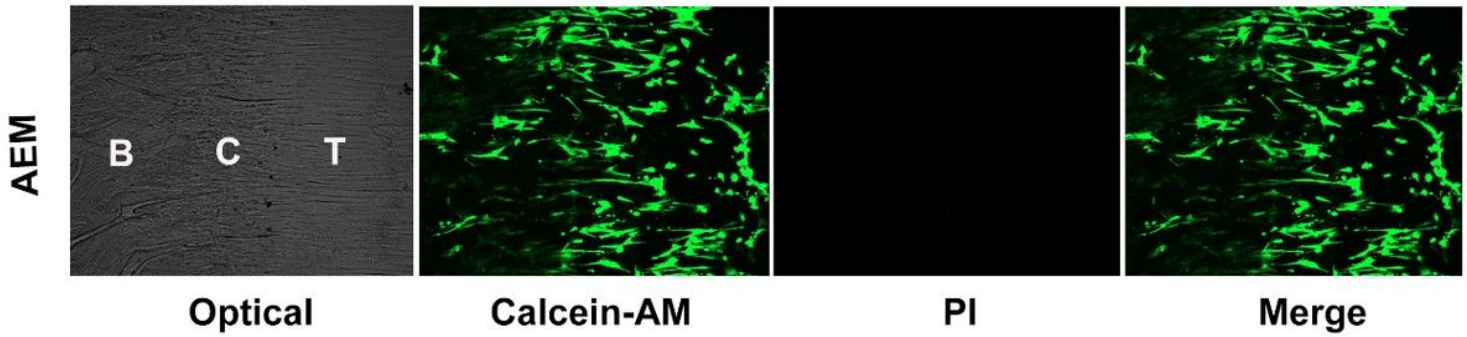

Figure 6

Live/dead cell analysis for the DEM on which hBMSCs seeded for 3 days. Representative images show the live (green) and dead (red) hBMSCs in the DEM (N=3). Bar = 100 μm.

Supplementary Files

This is a list of supplementary files associated with this preprint. Click to download.

- TheARRIVEGuidelinesChecklist.pdf